

UCLA

UCLA Previously Published Works

Title

Characteristics of Detected and Missed Prostate Cancer Foci on 3-T Multiparametric MRI Using an Endorectal Coil Correlated With Whole-Mount Thin-Section Histopathology.

Permalink

<https://escholarship.org/uc/item/8d79x3cn>

Journal

American Journal of Roentgenology, 205(1)

ISSN

0361-803X

Authors

Tan, Nelly
Margolis, Daniel J
Lu, David Y
[et al.](#)

Publication Date

2015-07-01

DOI

10.2214/ajr.14.13285

Peer reviewed



Published in final edited form as:

AJR Am J Roentgenol. 2015 July ; 205(1): W87–W92. doi:10.2214/AJR.14.13285.

Characteristics of Detected and Missed Prostate Cancer Foci on 3-T Multiparametric MRI Using an Endorectal Coil Correlated With Whole-Mount Thin-Section Histopathology

Nelly Tan¹, Daniel J. Margolis¹, David Y. Lu², Kevin G. King¹, Jiaoti Huang², Robert E. Reiter³, and Steven S. Raman^{1,3}

¹Department of Radiology, David Geffen School of Medicine at UCLA, Box 957437, RRUMC 1621, Los Angeles, CA 90095

²Department of Pathology, David Geffen School of Medicine at UCLA, Los Angeles, CA

³Department of Urology, David Geffen School of Medicine at UCLA, Los Angeles, CA

Abstract

OBJECTIVE—The objective of this study was to determine the characteristics of prostate cancer foci missed on 3-T multiparametric MRI performed with an endorectal coil.

MATERIALS AND METHODS—The MRI examinations of 122 patients who underwent 3-T multiparametric MRI of the prostate with an endorectal coil were compared with whole-mount histopathology obtained after radical prostatectomy. The mean age of the patients was 60.6 years (SD, 7.6 years), and the mean prostate-specific antigen value was 7.2 ng/mL (SD, 5.9 ng/mL). The clinical, multiparametric MRI (i.e., T2-weighted imaging, diffusion-weighted imaging, and dynamic contrast-enhanced imaging), and histopathologic features were obtained. After an independent review, two blinded genitourinary radiologists matched each case with a genitourinary pathologist. A structured reporting system was used to classify the multiparametric MRI features of each MRI-detected lesion. A chi-square analysis was performed for categorical variables, and the *t* test was performed for continuous variables.

RESULTS—On whole-mount histopathology, 285 prostate cancer foci were detected in 122 patients. Of the 285 cancer foci detected at histopathology, 153 (53.3%) were missed on MRI and 132 (46.7%) were detected on MRI. Of the missed lesions, 75.2% were low-grade prostate cancer. Multiparametric MRI had a significantly higher sensitivity for prostate cancer foci 1 cm or larger than for subcentimeter foci (81.1% vs 18.9%, respectively; $p < 0.001$), for lesions with a Gleason score of 7 or greater than for lesions with a Gleason score of 6 (72.7% vs 27.3%; $p < 0.01$), and for index lesions than for satellite lesions (80.3% vs 20.8%; $p < 0.01$). The 3-T multiparametric MRI examinations showed a higher detection rate for lesions in the midgland or base of the gland compared with lesions in the apex (52.3% vs 22.0%, respectively; $p < 0.01$).

CONCLUSION—Compared with the prostate cancer lesions that were detected on multiparametric MRI, the prostate cancer lesions that were missed were significantly smaller, were

more likely to be low-grade lesions (i.e., Gleason score of 6), were more commonly satellite lesions, and were more likely to be located in the prostatic apex.

Keywords

multiparametric prostate MRI; prostate cancer

Systematic 12-core transrectal ultrasound (TRUS) biopsy has been used as the standard of reference for the nonsurgical localization of prostate cancer and is endorsed by the American Urological Association [1]. However, standard TRUS-guided biopsies are nontargeted and have poor sensitivity for prostate cancer detection, ranging from 32% to 41%, and have poor sensitivity for the localization and characterization of the extent of disease [2, 3]. Interest in in-bore and image fusion MRI-guided biopsy for focal prostate cancer and also in emerging focal therapy for prostate cancer (laser, focused ultrasound) has significantly increased in response to the need for better detection, characterization, and localization of individualized prostate cancer foci [4].

Multiparametric MRI of the prostate—with its high spatial and temporal resolution to image and map the entire prostate gland with anatomic and functional information—is the leading noninvasive technique to potentially detect and characterize significant prostate cancer foci with a higher Gleason grade [4, 5]. On T2-weighted MRI, prostate cancer foci tend to be rounded areas of decreased signal intensity in both the high-signal-intensity peripheral zone and mixed-signal-intensity transition zone [6, 7]. Higher-grade foci tend to have rapid wash-in and washout on dynamic contrast-enhanced MRI (DCE-MRI) and restricted water movement on DWI [7]. Multiparametric MRI has considerable promise for the integrated morphologic and functional assessment of prostate cancer, but there are limited data to evaluate the features of prostate cancer foci that were missed on multiparametric MRI. We describe the accuracy of 3-T multiparametric MRI for the localization of prostate cancer and identify characteristics of prostate cancer missed on multiparametric MRI using histopathologic results of whole-mount preparations of specimens obtained at radical prostatectomy as the standard of reference.

Materials and Methods

Study Design and Population

In this HIPAA-compliant and institutional review board–approved study, we performed a single-institution study of 122 consecutive men who underwent 3-T multiparametric MRI before radical prostatectomy from October 2010 to January 2013. All patients had prior biopsy-proven prostate adenocarcinoma and underwent robot-assisted radical prostatectomy after MRI was performed. Exclusion criteria were contraindications to MRI (e.g., cardiac devices, prosthetic valves, severe claustrophobia) or significant technical limitations (e.g., artifacts from severe hemorrhage).

MRI

Multiparametric MRI was performed using an endorectal coil and an external phased-array coil on a 3-T magnet (Trio, Verio, or Skyra, Siemens Healthcare) in 108 of 122 (88.5%)

patients; the remaining patients underwent multiparametric MRI using an external phased-array coil for active surveillance screening without undergoing repeat multiparametric MRI examinations using an endorectal coil. The endorectal coil was inserted using a semianesthetic gel (benzocaine gel [Hurracaine, Beutlich Pharmaceuticals]) or nonanesthetic lubricant (Surgilube, Savage Laboratories) while the patient was in the left lateral decubitus position. The balloon was insufflated with 50 mL of perfluorocarbon (3 mol/L [Fluorinert, 3M]) to reduce susceptibility artifact from air. An anti-peristaltic agent (1 mg of glucagon) was administered intramuscularly to reduce bowel peristalsis.

The MRI protocol included T2-weighted turbo spin-echo (TSE), DWI, axial unenhanced T1-weighted, and axial 3D fast-field echo DCE-MRI sequences. A small-FOV 3D axial TSE T2-weighted sequence was performed using spatial and chemical-shift encoded excitation (SPACE, Siemens Healthcare) and the following parameters: TR range/TE, 3800–5040/101; echo-train length (ETL), 13; FOV, 14 cm; matrix, 256 × 256; and 1.5-mm contiguous slices. In addition, 2D axial and coronal TSE T2-weighted sequences were performed (TR range/TE, 3800–5040/101; ETL, 13; FOV, 14 × 14 cm; matrix, 256 × 205; slice thickness, 3 mm; no gap).

For the DWI sequence, echo-planar imaging was used with the following parameters: TR/TE, 3900/60; FOV, 21 × 26 cm; matrix, 130 × 160; slice thickness, 3.6 mm; and number of signals acquired, 4). The b values were 0, 100, 400, and 800 s/mm² with a calculated or natively acquired b value of 1400 s/mm².

A dynamic view-sharing time-resolved angiography with stochastic trajectories gradient-echo T1-weighted sequence was performed over 6 minutes (4.75 seconds per acquisition) with a 15-second injection delay (TWIST, Siemens Healthcare) The following parameters were used: TR/TE, 3.9/1.4; flip angle, 12°; FOV, 26 × 26 cm; matrix, 160 × 160; and slice thickness, 3.6 mm. For this sequence, image analysis was performed using VersaVue (iCAD).

A diffusion-tensor imaging sequence was performed using a twice-refocused echo-planar acquisition and the following parameters: TR/TE, 5599/137; ETL, 36; FOV, 26 cm; matrix, 128 × 96; slice spacing, 3.6 mm; and number of signals acquired, 1. For this sequence, 12–30 noncolinear diffusion-sensitizing directions with b values of 0 and 600 mm/s² or higher were used, or 30 directions with b values of 800, 1500, and 4000 mm/s² were used. Either VersaVue or DynaCAD (version 3, Invivo) was used for 3D volume-of-interest delineation and pharmacokinetic analysis. ROIs were drawn separately on the apparent diffusion coefficient map and perfusion images to accommodate any image offset and distortion between the T2-weighted and functional series.

MRI and Histopathologic Analysis and Correlation

Two fellowship-trained genitourinary radiologists with 8 and 12 years of experience in prostate MRI, respectively, identified prostate cancer lesions on preoperative multiparametric MRI. Lesions were then characterized for aggressiveness using a standardized system [8]. Briefly, the standardized classification system consisted of scoring each parameter (T2-weighted imaging, DWI, DCE-MRI) on a Likert scale ranging from 1 to

5; the highest possible total score was 15 (5 points for each of the three parameters). More than mild clinical suspicion, defined as a total score of 5 or greater by consensus, was considered a suspicious lesion. The degree of postbiopsy hemorrhage was also graded on a Likert scale ranging from 1 to 5: Severe hemorrhage was defined as a score of 4 or 5, and 1 was defined as no hemorrhage.

Histopathologic examinations of the whole-mount thin-section preparations of the specimens obtained at radical prostatectomy were performed by a dedicated genitourinary pathologist. On each section, individual prostate cancer lesion size, location, and Gleason pattern were given. In a series of sessions, both multiparametric MRI and histopathologic examinations were rereviewed individually by both genitourinary radiologists and by two genitourinary pathologists (Fig. 1). Individual prostate cancer lesions were detected and characterized on both histopathologic and MRI examinations as discussed earlier. The index lesion was defined as the largest and highest-grade prostate cancer lesion. A satellite lesion was defined as a nonindex lesion (i.e., multifocal lesions that had lower grade or were smaller than the index lesion). Based on these analyses, the sensitivity, positive predictive value (PPV), and false-negative rates of multiparametric MRI were calculated.

Statistical Analysis

Chi-square analysis was performed for categorical variables, and the *t* test was performed for continuous variables. All statistical analyses were performed using statistics software (Stata, version 11.2, StataCorp). All *p* values correspond to a two-sided test, and a *p* value < 0.05 was considered statistically significant.

Results

Histologic Findings

The study cohort included 285 prostate cancer foci detected on whole-mount histopathologic examinations in 122 patients. The mean age of the study cohort was 60.6 years (SD, 7.6 years), and the mean prostate-specific antigen (PSA) value was 7.2 ng/mL (SD, 5.9 ng/mL). On 3-T multiparametric MRI, 152 (53.3%) prostate cancer foci were missed and 132 (46.7%) prostate cancer foci were detected. Of the missed lesions, there were 115 lesions (75.2%) with a Gleason score of 3 + 3, 23 (15.0%) with a Gleason score of 3 + 4, nine (5.9%) with a Gleason score of 4 + 3, and six (3.9%) with a Gleason score of 8–10 (Table 1). The majority of patients had multiple prostate cancer foci on histopathologic examination: 30 patients (24%) had two foci and 49 (39.8%) had three or more foci, whereas 44 (36.1%) had a solitary tumor and the remainder had multifocal tumors (Table 1). Of the 279 prostate cancer foci, 220 (78.9%) prostate cancer foci were at the midgland or base and the remaining 59 (21.1%) were apical. Most patients had pT2 tumors (87 patients [71.3%]), and the remaining patients had pT3 lesions (pT3a, 30 [24.6%]; pT3b, 5 [4.1%]). There was no difference in the preoperative PSA values of tumors detected and those not detected on 3-T multiparametric MRI. When the study group was stratified by index lesions, 98 of 122 (80.3%) index lesions were detected. Of the 44 solitary tumors, 39 (88.6%) were identified on multiparametric MRI.

On univariate analysis, of 154 (54.0%) prostate cancer foci that were 1 cm or larger at pathology, 107 (69.5%) were detected on 3-T multiparametric MRI and 47 (30.5%) were missed ($p < 0.01$). Ninety-six of 132 (72.7%) prostate cancer lesions with a Gleason score of 3 + 4 or greater were detected on multiparametric MRI and 36 of 151 (23.8%) low-grade lesions were detected on multiparametric MRI; in other words, 115 (75.2%) prostate cancer lesions with a Gleason score of 3 + 3 were missed on multiparametric MRI ($p < 0.01$) (Fig. 2). Our results showed that a significantly greater proportion of intermediate- to high-grade lesions were detected on 3-T multiparametric MRI (Fig. 3) for both index and satellite prostate cancer foci compared with low-grade lesions. The location of the tumor also impacted detection on MRI. More prostate cancer lesions located in the midgland or base of the gland were detected on 3-T multiparametric MRI than apical lesions (52.3% vs 22.0%, respectively; $p < 0.01$) (Table 2 and Fig. 4).

MRI Findings

Multiparametric MRI had significantly higher sensitivity for prostate cancer foci 1 cm or larger than for subcentimeter prostate cancer foci (107/154 [69.5%] vs 25/131 [19.1%], respectively; $p < 0.001$), lesions with a Gleason score of 7 or greater than for lesions with a Gleason score of 6 (96/132 [72.7%] vs 36/132 [27.3%]; $p < 0.01$), and index lesions than for satellite lesions (98/122 [80.3%] vs 34/163 [20.8%]; $p < 0.01$). Sensitivity of 3-T multiparametric MRI for detection of all prostate cancer foci was 46.3%, of lesions 1 cm or larger was 69.5%, of lesions with a Gleason score of 7 or greater was 72.7%, and of index lesions was 80.3% (Table 3). On a per-patient analysis, the false-negative rate of multiparametric MRI was 19.7% (24/122 patients) (Table 2). A subanalysis of this group with false-negative MRI findings showed that there was a significant difference in the proportion of patients who had severe hemorrhage between the group with false-negative MRI findings (13/24 [54.2%]) and the group with true-positive MRI findings (34/98 [34.7%]) ($p = 0.02$). Moreover, the positive predictive value (PPV) of multiparametric MRI was 74.6% (132/177). In other words, of the 177 lesions that were detected on MRI, 45 (25.4%) were overcalled (i.e., false-positive findings).

Discussion

In this study, we performed a careful review of 3-T multiparametric MRI and whole-mount histopathologic examinations (Fig. 5) to determine the characteristics of the prostate cancer foci that were missed on 3-T multiparametric MRI. Using the histopathologic examinations of whole-mount preparations of specimens obtained at radical prostatectomy as the ground truth compared with the lesions identified on multiparametric MRI provides the highest degree of rigor excluding a mold-based inherently coregistered whole-mount histopathologic technique [⁹]. The results of our study show that the prostate cancer lesions that were missed on multiparametric MRI were smaller, were more likely to be low-grade prostate cancer (Gleason score 3 + 3), were satellite lesions more often, and were more commonly located at the prostatic apex. These results corroborate the results of prior work suggesting that prostate multiparametric MRI is effective at detecting index and solitary lesions, lesions located in the midgland and base of the prostate, lesions with intermediate- or high-grade

prostate cancer, and lesions that are solitary or dominant. These findings support the concept that multiparametric MRI may be useful for localizing index solitary lesions [10].

The prostate apex is a common location of tumor involvement: 35–80% of tumors extend into the prostate apex [11, 12]. Consistent with results reported by other investigators [13], we also found that the sensitivity of multiparametric MRI for prostate cancer in the prostate apex is significantly less than in the midgland or base. The specificity of multiparametric MRI for prostate cancer in the apex is a recognized limitation of T2-weighted imaging. Low signal intensity on T2-weighted imaging in the peripheral zone is the primary indicator of prostate tumor but can also be caused by inflammation, postbiopsy hemorrhage, and postradiation changes. It appears that both the detection and resection of apical lesions are challenging. The apical capsule is less conspicuous both on imaging and at resection, and periprostatic fat is usually sparse or completely absent in the apex, which may make the tumor less visible. Positive surgical margins in the apical region are found in 7–62% of prostatectomies [11, 14, 15]. However, although positive margins at the apex are common, studies in the literature suggest that a single positive apical margin may be clinically insignificant [12, 16]. A multivariate analysis of 2334 cases of organ-confined cancer showed that only positive margins at the prostate base were significantly associated with an increased risk of biochemical failure [16]. Apical, anterior midgland, and posterior midgland prostate margins do not impart a worse prognosis on multivariate analysis [16]. These findings suggest that the limited detection of apical lesions may not have a significant clinical impact for biochemical recurrence after surgery compared with lesions in the midgland or in the base of the gland. However, if local regional thermal ablation options are considered, our study suggests that we need to be mindful of the apex, where clinically significant lesions may be missed. The results of our study suggest that additional attention to this region is needed in these cases.

In our study, a majority of the satellite tumors were missed on MRI. Noguchi et al. [17] evaluated the impact of satellite tumors on PSA recurrence after prostatectomy. They stratified their patients into three groups according to tumor focality (single vs multiple) and secondary cancer volume, including a single tumor, an index (largest) tumor with secondary tumors less than 0.5 mL, and an index tumor with secondary tumors greater than 0.5 mL. Comparison of PSA failure rates among the three groups, the multifocal group with smaller secondary cancers showed a better prognosis than the group with a single tumor ($p = 0.019$). Their findings suggested that secondary cancers in multifocal prostate tumors did not adversely influence the performance of preoperative clinical parameters, including PSA and needle biopsy. In fact, the percentages of Gleason patterns 4 and 5 cancers in the biopsies and prostatectomy specimens were the most powerful predictors of biochemical failure in men with stage Ic prostate cancer after prostatectomy. These results suggest that the lower detection rate of secondary tumors compared with solitary and index tumors in our population may not have a significant impact in oncologic outcomes. Instead, identification of the solitary or the index lesion may be the most important predictor of PSA recurrence.

In the background of multifocal and multiclonal primary prostate cancer, metastatic prostate cancers have monoclonal origins [18]. This characteristic of prostate cancers suggests that detection of a solitary tumor or an index tumor is the most clinically important purpose of

prostate multiparametric MRI. In our population, of the clinically significant tumors, 71.6% of tumors with a Gleason score of 7 or greater and 69.5% of lesions that were 1 cm or larger were detected. Similarly, Rosenkrantz et al. [19] reported an average sensitivity of 75.9% in an approximate match analysis for index lesions in a multireader setting. Their findings combined with the findings from this study suggest that if multiparametric MRI is to be used to identify patients who may be candidates for local tumor ablation of index lesions, multiparametric MRI may be effective for identifying the majority of the cases. However, index lesions were missed in 19.7% of patients in our patient population, which underscores the need for follow-up of men with clinical findings suggestive of prostate cancer but without definitive imaging evidence of worrisome lesions on multiparametric MRI.

There are limitations to this study. First, this study was retrospective and thus has intrinsic selection bias based on the study design. Second, this study was a single-institution experience, and these results may not be widely applicable. Third, we evaluated men who underwent radical prostatectomy and excluded men who underwent active surveillance or radiation therapy. Therefore, our findings may not reflect the population of men with prostate cancer who did not undergo surgery. Fourth, the intra- and interobserver variabilities cannot be measured because the study was based on consensus of two radiologists. Fifth, the test-retest reproducibility of the MRI examinations is unknown because no repeat MRI examinations were performed. Sixth, we did not routinely image the ex vivo prostate after prostatectomy and we did not use a prostate mold; therefore, the MRI scans and the whole-mount histopathologic slices were not directly superimposed.

Despite these limitations, this study is the first, to our knowledge, to evaluate the characteristics of tumors missed by state-of-the-art 3-T multiparametric prostate MRI on a per-lesion analysis in a high-volume institution using whole-mount histopathologic results as the reference standard. Moreover, to our knowledge, this study is the first to include and elucidate in-depth the relationship between tumor detection as a function of grade stratified by size, multifocality, and location using a per-lesion analysis. Although multiparametric prostate MRI has made significant advances, our findings show that multiparametric MRI has certain limitations about which we should be aware: Prostate cancer in the prostatic apex, low-grade tumors, and subcentimeter tumors are commonly missed on multiparametric MRI.

Acknowledgments

We thank Ely Felker and Stephanie Lee-Felker for critical review of the manuscript.

Supported by National Cancer Institute National Institutes of Health award P50CA092131 and Prostate Specialized Program of Research Excellence (SPORE).

D. J. Margolis received a grant from Siemens Healthcare.

References

1. Taneja SS, Bjurlin M, Carter HB, et al. American Urological Association website. AUA/optimal techniques of prostate biopsy and specimen handling. www.auanet.org/common/pdf/education/clinical-guidance/Prostate-Biopsy-WhitePaper.pdf. Published 2013.

2. Welch HG, Fisher ES, Gottlieb DJ, Barry MJ. Detection of prostate cancer via biopsy in the Medicare- SEER population during the PSA era. *J Natl Cancer Inst.* 2007; 99:1395–1400. [PubMed: 17848671]
3. Bjurlin MA, Carter HB, Schellhammer P, et al. Optimization of initial prostate biopsy in clinical practice: sampling, labeling and specimen processing. *J Urol.* 2013; 189:2039–2046. [PubMed: 23485507]
4. Murphy G, Haider M, Ghai S, Sreeharsha B. The expanding role of MRI in prostate cancer. *AJR.* 2013; 201:1229–1238. [PubMed: 24261361]
5. Boonsirikamchai P, Choi S, Frank SJ, et al. MR imaging of prostate cancer in radiation oncology: what radiologists need to know. *RadioGraphics.* 2013; 33:741–761. [PubMed: 23674772]
6. Hedgire SS, Eberhardt SC, Borczuk R, McDermott S, Harisinghani MG. Interpretation and reporting multiparametric prostate MRI: a primer for residents and novices. *Abdom Imaging.* 2014; 39:1036–1051. [PubMed: 24566965]
7. Hoeks CM, Barentsz JO, Hambroek T, et al. Prostate cancer: multiparametric MR imaging for detection, localization, and staging. *Radiology.* 2011; 261:46–66. [PubMed: 21931141]
8. Sonn GA, Chang E, Natarajan S, et al. Value of targeted prostate biopsy using magnetic resonance-ultrasound fusion in men with prior negative biopsy and elevated prostate-specific antigen. *Eur Urol.* 2014; 65:809–815. [PubMed: 23523537]
9. Trivedi H, Turkbey B, Rastinehad AR, et al. Use of patient-specific MRI-based prostate mold for validation of multiparametric MRI in localization of prostate cancer. *Urology.* 2012; 79:233–239. [PubMed: 22202553]
10. Ahmed HU, Hindley RG, Dickinson L, et al. Focal therapy for localised unifocal and multifocal prostate cancer: a prospective development study. *Lancet Oncol.* 2012; 13:622–632. [PubMed: 22512844]
11. Stamey TA, Villers AA, McNeal JE, Link PC, Freiha FS. Positive surgical margins at radical prostatectomy: importance of the apical dissection. *J Urol.* 1990; 143:1166–1172. discussion 1172–1173. [PubMed: 2342177]
12. Ohori M, Abbas F, Wheeler TM, Kattan MW, Scardino PT, Lerner SP. Pathological features and prognostic significance of prostate cancer in the apical section determined by whole mount histology. *J Urol.* 1999; 161:500–504. [PubMed: 9915435]
13. Wefer AE, Hricak H, Vigneron DB, et al. Sextant localization of prostate cancer: comparison of sextant biopsy, magnetic resonance imaging and magnetic resonance spectroscopic imaging with step section histology. *J Urol.* 2000; 164:400–404. [PubMed: 10893595]
14. Rosen MA, Goldstone L, Lapin S, Wheeler T, Scardino PT. Frequency and location of extracapsular extension and positive surgical margins in radical prostatectomy specimens. *J Urol.* 1992; 148:331–337. [PubMed: 1635129]
15. van den Ouden D, Bentvelsen FM, Boevé ER, Schröder FH. Positive margins after radical prostatectomy: correlation with local recurrence and distant progression. *Br J Urol.* 1993; 72:489–494. [PubMed: 7505193]
16. Blute ML, Bostwick DG, Bergstralh EJ, et al. Anatomic site-specific positive margins in organ-confined prostate cancer and its impact on outcome after radical prostatectomy. *Urology.* 1997; 50:733–739. [PubMed: 9372884]
17. Noguchi M, Stamey TA, McNeal JE, Nolley R. Prognostic factors for multifocal prostate cancer in radical prostatectomy specimens: lack of significance of secondary cancers. *J Urol.* 2003; 170:459–463. [PubMed: 12853799]
18. Liu W, Laitinen S, Khan S, et al. Copy number analysis indicates monoclonal origin of lethal metastatic prostate cancer. *Nat Med.* 2009; 15:559–565. [PubMed: 19363497]
19. Rosenkrantz AB, Deng FM, Kim S, et al. Prostate cancer: multiparametric MRI for index lesion localization—a multiple-reader study. *AJR.* 2012; 199:830–837. [PubMed: 22997375]

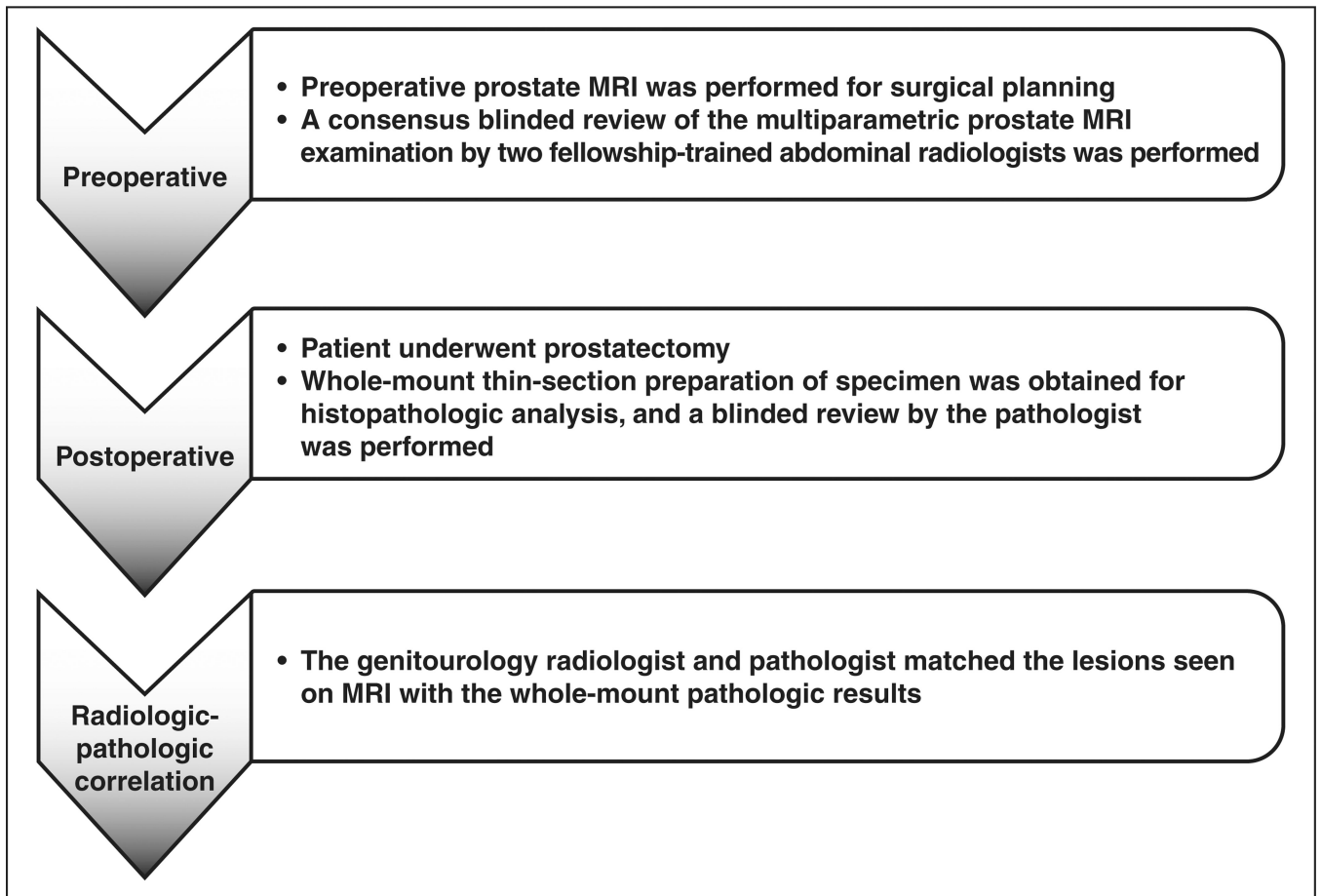


Fig. 1. Graphic shows sequence of tasks for radiologic-pathologic review process used for this study.

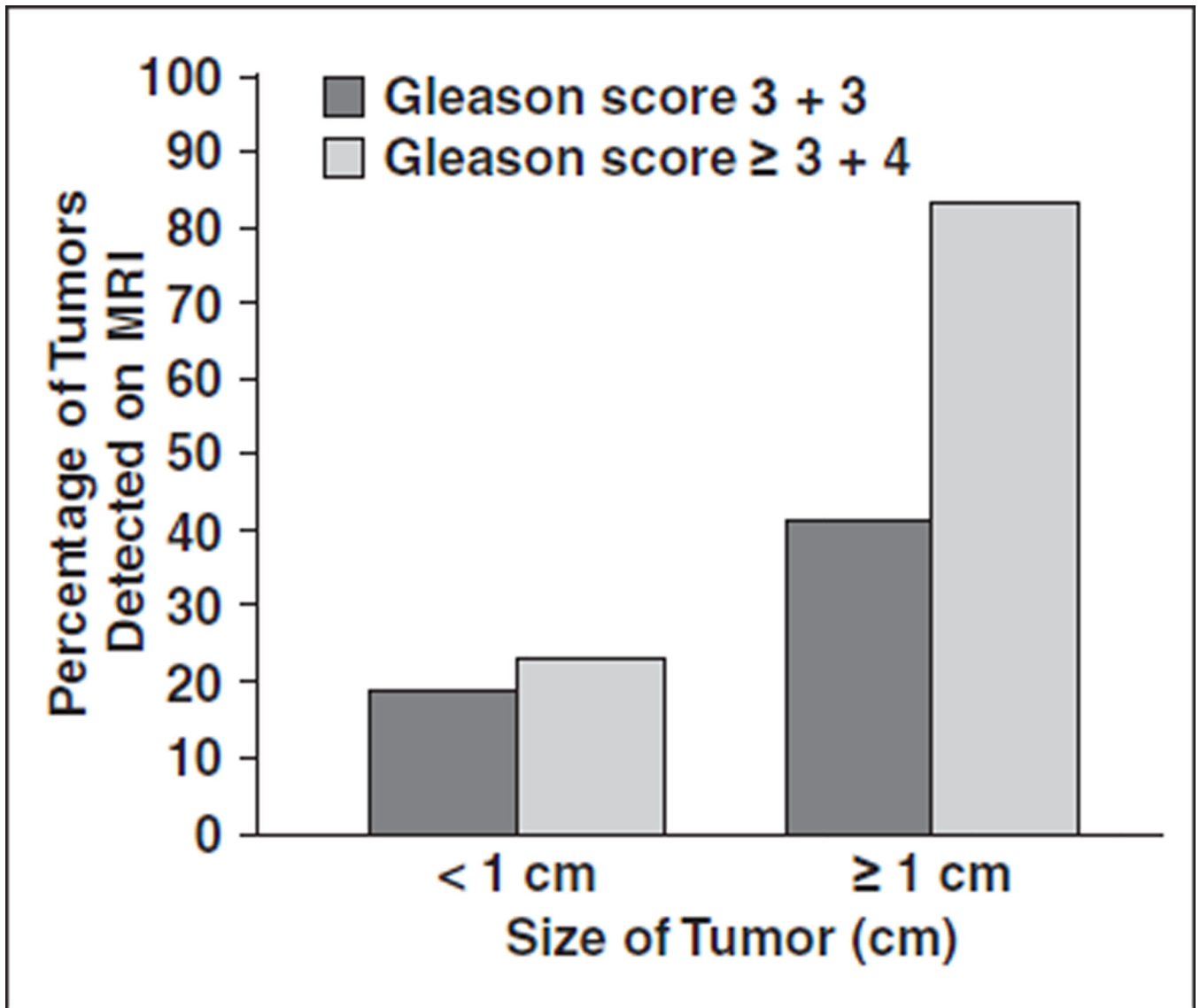


Fig. 2. Bar graph shows percentage of prostate tumors detected on MRI stratified by tumor size and by sum of Gleason scores ($p < 0.01$).

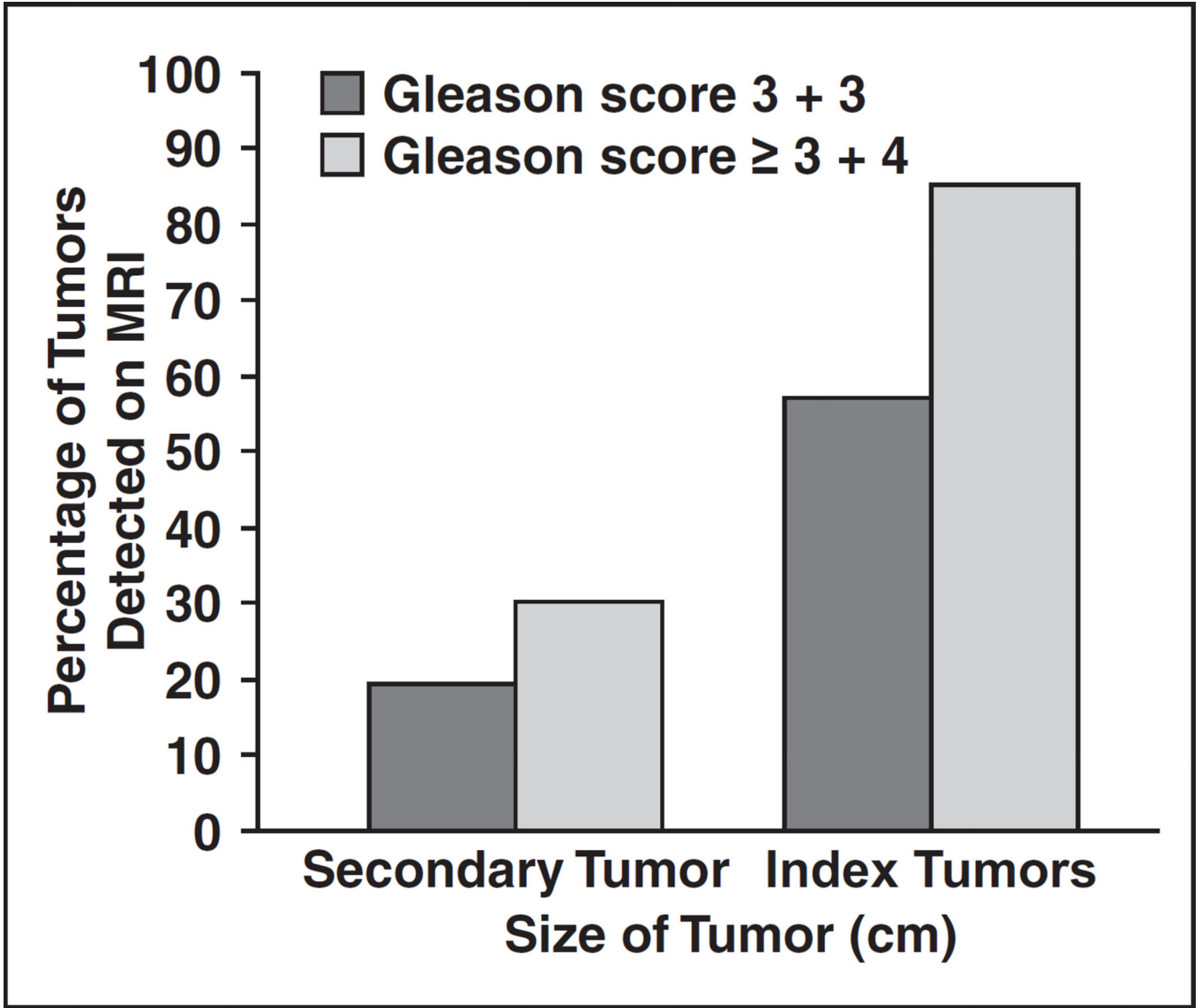


Fig. 3. Bar graph shows percentage of prostate tumors detected on MRI stratified by index tumors (vs secondary tumors) and by Gleason score ($p < 0.01$).

Author Manuscript

Author Manuscript

Author Manuscript

Author Manuscript

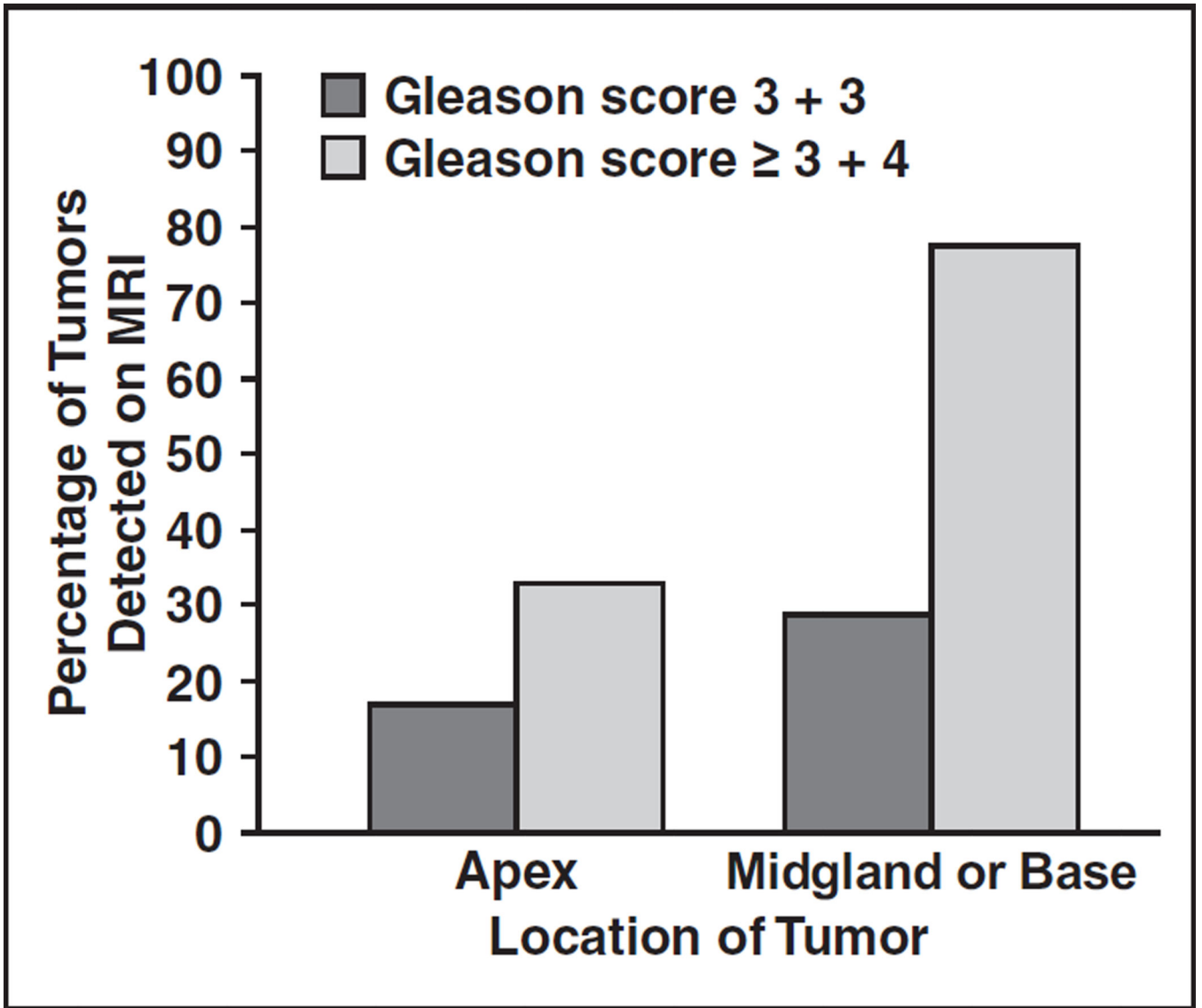


Fig. 4. Bar graph shows percentage of prostate tumors detected on MRI stratified by location and by Gleason score ($p < 0.01$).

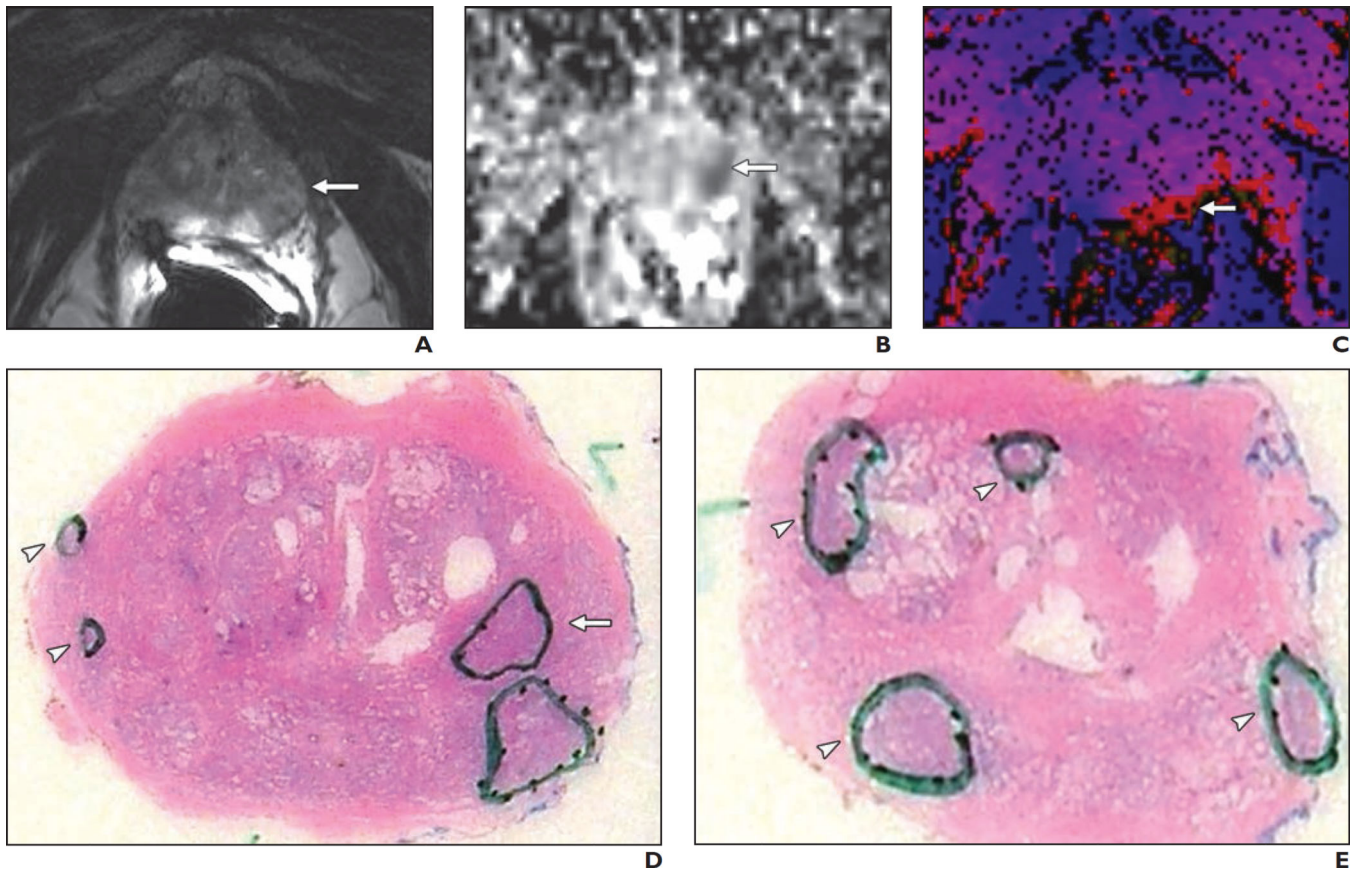


Fig. 5.

67-year-old man with elevated prostate-specific antigen value.

A, T2-weighted image shows hypointense lesion (*arrow*) in left peripheral zone.

B, Diffusion-weighted image shows diffusion restriction (*arrow*) in area corresponding to hypointense lesion on T2-weighted image (**A**).

C, Dynamic contrast-enhanced MR image shows perfusion abnormality (*arrow*) in area corresponding to hypointense lesion on T2-weighted image (**A**).

D and **E**, Patient underwent robot-assisted laparoscopic prostatectomy. Photomicrographs of thin sections from whole-mount preparation of specimen obtained at radical prostatectomy show index lesion (*arrow*, **D**) with Gleason score of 3 + 4 that corresponds to lesion shown by multiparametric MRI. However, multiple subcentimeter lesions with Gleason score of 3 + 3 (*arrowheads*) in right midgland and apex were missed on multiparametric MRI.

TABLE 1

Clinical and Pathologic Characteristics of Study Cohort

Characteristics	Value
Patients, no.	122
PSA (ng/mL), mean (SD)	7.2 (5.9)
All tumors, no.	285
Index tumors, no.	122
Tumor diameter (cm), mean (SD)	1.3 (0.99)
No. of tumors per patient, no. (%) of patients	
1	44 (36.1)
2	29 (23.8)
3	24 (19.7)
4	25 (20.5)
Gleason score, no. (%) of tumors	
6	151 (53.0)
3 + 4	77 (27.0)
4 + 3	38 (13.3)
8–10	19 (6.7)
T stage, no. (%) of patients	
T2	87 (71.3)
T3a	30 (24.6)
T3b	5 (4.1)

Note—PSA = prostate-specific antigen.

TABLE 2

Differences in Characteristics Between Prostate Tumors Detected and Those Missed on Multiparametric MRI

Characteristics	Positive MRI Findings and Positive Histopathologic Results	Negative MRI Findings and Positive Histopathologic Results	Total	<i>p</i>
Detection of tumors, no. (%) of tumors				< 0.01
Index lesions	98 (80.3)	24 (19.7)	122 (100.0)	
Satellite tumors	34 (20.8)	129 (79.1)	163 (100.0)	
Total	132 (46.7)	153 (53.3)	285 (100.0)	
PSA (ng/mL), mean (SD)	7.7 (7.2)	7.1 (5.4)	7.2 (5.9)	0.44
Tumor diameter, no. (%) of tumors				< 0.001
< 1 cm	25 (19.1)	106 (80.9)	131 (100.0)	
1 cm	107 (69.5)	47 (30.5)	154 (100.0)	
Total	132 (53.7)	153 (46.3)	285 (100.0)	
Gleason score, no. (%) of tumors (<i>n</i> = 285)				< 0.01
6	36 (27.3)	115 (75.2)	151 (53.0)	
3 + 4	54 (40.9)	23 (15.0)	77 (27.0)	
4 + 3	29 (22.0)	9 (5.9)	38 (13.3)	
8–10	13 (9.8)	6 (3.9)	19 (6.7)	
Total	132 (100.0)	153 (100.0)	285 (100.0)	
Location of tumors, no. (%) of tumors (<i>n</i> = 279)				< 0.01
Apex	13 (22.0)	46 (78.0)	59 (100.0)	
Midgland or base	115 (52.3)	105 (47.7)	220 (100.0)	
Total	128 (45.9)	151 (54.1)	279 (100.0)	

Note—PSA = prostate-specific antigen.

TABLE 3

Sensitivities and Positive Predictive Values (PPVs) of MRI Detection of All Tumors, Tumors ≥ 1 cm, Tumors With a Gleason Score of ≥ 7 , Index Lesions, and Satellite Lesions

MRI Detection of	Sensitivity	PPV
All tumors	132/285 (46.3)	132/177 (74.6)
Tumors ≥ 1 cm	107/154 (69.5)	107/152 (70.4)
Tumors with a Gleason score ≥ 7	96/132 (72.7)	96/141 (68.1)
Index lesions	98/122 (80.3)	98/98 (100.0)
Satellite lesions	34/163 (20.8)	34/79 (43.0)

Note—Data are presented as no. of tumors detected on MRI/total no. of tumors (%).

Author Manuscript

Author Manuscript

Author Manuscript

Author Manuscript